Heliyon 6 (2020) e04207

Contents lists available at ScienceDirect

Heliyon

journal homepage: www.cell.com/heliyon

Research article

Analysis of the variability of airborne particulate matter with prevailing meteorological conditions across a semi-urban environment using a network of low-cost air quality sensors

Opeyemi R. Omokungbe [a], Olusegun G. Fawole [a,b,*], Oyediran K. Owoade [a], Olalekan A.M. Popoola [c], Roderic L. Jones [c], Felix S. Olise [a], Muritala A. Ayoola [a], Pelumi O. Abiodun [a], Adekunle B. Toyeje [a], Ayodele P. Olufemi [d], Lukman A. Sunmonu [a], Olawale E. Abiye [e]

[a] Environmental Pollution Research Laboratory, Department of Physics and Engineering Physics, Obafemi Awolowo University, Ile-Ife 230001, Nigeria
[b] Atmospheric Science Unit, Department of Environmental Sciences, Stockholm University, SE-11418 Stockholm, Sweden
[c] Department of Chemistry, University of Cambridge, Cambridge, CB2 1EW, UK
[d] Department of Physics, University of Medical Sciences, Ondo, Nigeria
[e] Centre for Energy Research and Development (CERD), Obafemi Awolowo University, Ile-Ife, Nigeria

ARTICLE INFO

Keywords:
Low-cost AQ sensors
Meteorological variables
Particulate matter
Multiple linear regression (MLR)
RMSE
Iron smelter
Atmospheric science
Environmental analysis
Environmental assessment
Environmental impact assessment
Environmental pollution

ABSTRACT

The concentrations of fine and coarse fractions of airborne particulate matter (PM) and meteorological variables (wind speed, wind direction, temperature and relative humidity) were measured at six selected locations in Ile Ife, a prominent university town in Nigeria using a network of low-cost air quality (AQ) sensor units. The objective of the deployment was to collate baseline air quality data and assess the impact of prevailing meteorological conditions on PM concentrations in selected residential communities downwind of an iron smelting facility. The raw data obtained from OPC-N2 of the AQ sensor units was corrected using the RH correction factor developed based k-Kohler theory. This PM (corrected) fast time resolution data (20 s) from the AQ sensor units were used to create daily averages. The overall mean mass concentrations for $PM_{2.5}$ and PM_{10} were 213.3, 44.1, 23.8, 27.7, 20.2 and 41.5 μg/m^3 and; 439.9, 107.1, 55.0, 72.4, 45.5 and 112.0 μg/m^3 for Fasina (Iron-Steel Smelting Factory, ISSF), Modomo, Eleweran, Fire Service, O.A.U. staff quarters and Obafemi Awolowo University Teaching and Research Farm (OAUTRF), respectively. PM concentration and wind speed showed a negative exponential distribution curve with the lowest exponential fit coefficient of determination (R^2) values of 0.08 for $PM_{2.5}$ and 0.03 for PM_{10} during nighttime periods at Eleweran and Fire service sites, respectively. The relationship between PM concentration and temperature gave a decay curve indicating that higher PM concentrations were observed at lower temperatures. The exponential distribution curve for the relationship between PM concentration and relative humidity (RH) showed that PM concentrations do not vary for RH < 80 % while stronger relationship was noticed with higher PM concentration for RH > 80 % for both day and nighttime. The performances of the MLR model were slightly poor and as such not too reliable for predicting the concentration but useful for improving predictive model accuracy when other variables contributing to the variability of PM is considered. The study concluded that the anthropogenic and industrial activities at the smelting factory contribute significantly to the elevated PM mass concentration measured at the study locations.

Main findings

As far as 6 – 8 km downwind, the iron smelter is the prominent source of PM. A significant impact of RH on PM mass concentration was observed at a threshold of RH > 80 %. Considering their low cost and the performances assessed in this study, a justifiable conclusion is that low-cost optical particle counter (OPC-N2) has significant potential for implementing a dense network for air quality monitoring, especially in developing economies. Meteorological variables account more for $PM_{2.5}$ concentration than PM_{10} concentrations.

* Corresponding author.
E-mail address: pharwarlay@yahoo.com (O.G. Fawole).

https://doi.org/10.1016/j.heliyon.2020.e04207
Received 25 November 2019; Received in revised form 13 February 2020; Accepted 10 June 2020

Table 1. Description of the sampling sites.

Site	Co-ordinates	Site Description
Fasina (ISSF)	7.30° N, 4.28° E	Close to the main road and opposite iron smelting industry
Modomo	7.29° N, 4.29° E	Residential area close to the main road and downwind of iron smelter
Eleweran	7.30° N, 4.29° E	Residential area further away from iron smelter and main road
Fire Service Station	7.30° N, 4.31° E	OAU campus area directly opposite the main road on the university campus
Staff Quarters	7.31° N, 4.31° E	OAU Staff residential area with few anthropogenic PM sources
Teaching and Research Farm (OAUTRF)	7.33° N, 4.33° E	Area dedicated to agricultural activities including planting and rearing of animals

1. Introduction

Particulate matter (PM) exists as discrete particles such as liquid droplet or solids over a wide range of sizes (Seinfeld and Pandis, 2016). PM can be emitted directly into the atmosphere (primary particles) or they can be formed in the atmosphere (secondary particles) via physico-chemical transformations of the primary particles emitted from various anthropogenic and natural sources (Seinfeld and Pandis, 2016; Sumesh et al., 2017). In urban settings, especially in developing nations such as Nigeria, major sources of PM are combustion of fossil fuels (traffic and heavy-duty power generating sets), household cooking, biomass and refuse burning, industrial activities, smelting and other energy generation processes (Owoade et al., 2016). Long-term exposure to high concentrations of $PM_{2.5}$ has been associated with severe health impacts including stroke, ischemic heart disease, chronic obstructive pulmonary disease, lung cancer and acute lower respiratory infection (Lin et al., 2016). PM are grouped into various fractions depending on their aerodynamic diameter (D_{ae}), which is a unit density sphere with identical characteristics (Sturm, 2012). The two fractions of PM that has been extensively studies are $PM_{2.5}$ (fine - $D_{ae} \leq 2.5$ μm) and PM_{10} (coarse - $D_{ae} \leq 10$μm) (Harrison, 2014). Windborne dust, sea spray, volcanic eruptions, terrestrial dust, soil re-suspension, and biological particles are major natural sources of PM while anthropogenic sources include fossil fuel power plants, biomass burning, construction, quarrying and mining (Harrison, 2015; Seinfeld and Pandis, 2016). Fine fractions of PM are produced mainly from combustion processes, chemical reactions among reactive gaseous pollutants and coagulation of smaller particle sizes (Ancelet et al., 2011).

Ambient concentration of PM varies greatly; apart from source strength, it is majorly influenced by weather patterns and meteorological conditions (Owoade et al., 2012). Processes such as transportation, chemical transformation and removal mechanism of aerosol from the atmosphere are also influenced by meteorological conditions (Mohan, 2016). In the lower atmosphere, especially the atmospheric boundary layer, chemical composition, concentration, residence time and removal rate of atmospheric PM are greatly influence by prevailing meteorological conditions (Sumesh et al., 2017). Globally, several studies (for example, Jayamurugan et al. (2013); Owoade et al. (2012); Zu et al. (2017)) have been carried out to study and assess the relationship between PM concentration and meteorological variable such as wind speed, wind direction, relative humidity, air temperature, rain fall e.t.c. The study by Żyromski et al. (2014) focused on the relationship between the concentration of air pollutants and meteorological variables using linear and non-linear regression models. Several studies have reported the existence of varying degrees of correlations between air pollutants concentration and meteorological variables. Many of these studies, for example, Chakraborty et al. (2016); Chakraborty et al. (2018); Galindo et al. (2011); Haque et al. (2016); Hu et al. (2018), have identified meteorology as a major determinant of ambient PM concentrations since dispersion processes, removal mechanisms and chemical formation of atmospheric particles depend on parameters such as wind speed, rainfall rate, and solar radiation. The advection and dispersion of PM from

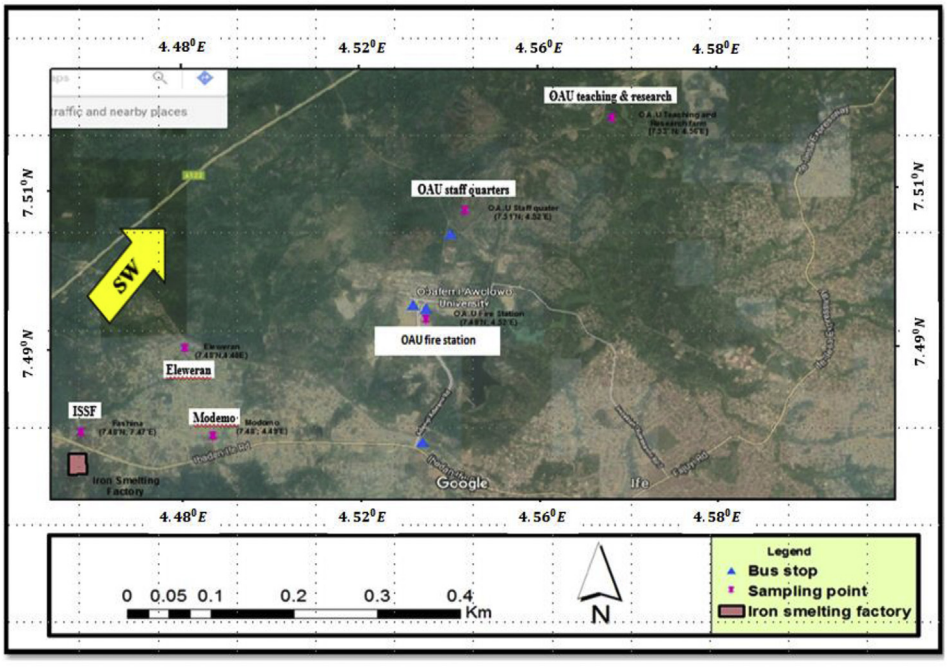

Figure 1. Google Earth map showing the study locations in Ile-Ife. The Yellow arrow indicates the prevailing wind direction.

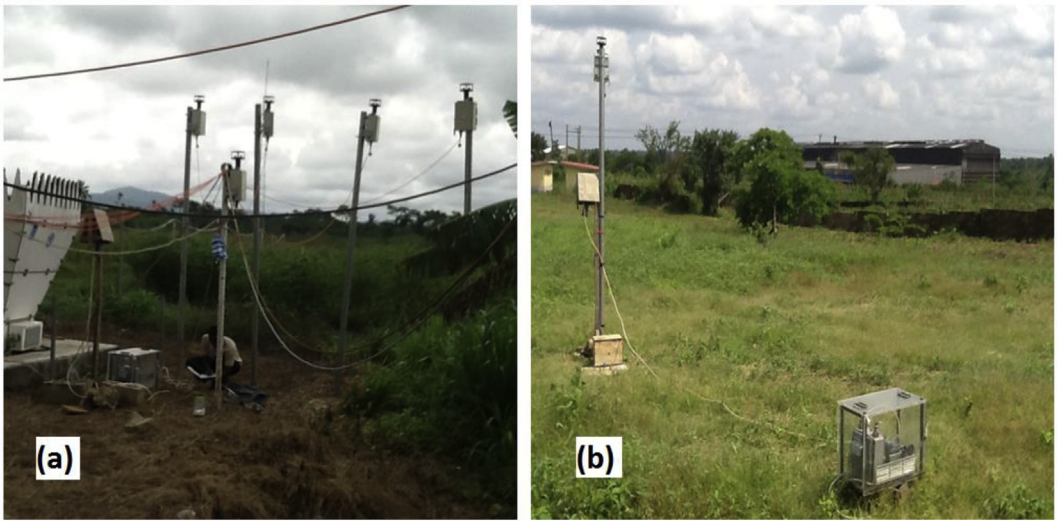

Figure 2. Field deployment of SNAQ units (a) Collocation of the SNAQ units at OAUTRF (b) SNAQ unit and Gent sampler with the iron smelter in the background.

anthropogenic sources could be enhanced by prevailing meteorology (Gogikar et al., 2018; Mahapatra et al., 2018).

One of the loss mechanisms of PM within the boundary layer is dry deposition through gravitational sedimentation. For coarse mode particle, from diameter >2.5 μm, the atmospheric residence time is shorter because they have larger sedimentation velocities and as such settle out of the atmosphere faster. The removal mechanism responsible for the sedimentation of the coarse mode fraction in the atmosphere is inefficient in the accumulation mode. As such, particles in the accumulation mode tends to have longer residence time (Seinfeld and Pandis, 2016). Owoade et al. (2012), using a high volume Gent sampler, measured PM mass concentration and established good correlations between PM concentrations and meteorological parameters at a site in Ile-Ife, Nigeria. Results from just one location might not give a good representation of the variation of PM concentration with meteorological variables over an entire study area.

The objectives of the present study are: (i) measure and assess ambient concentrations of PM and basic meteorological parameters using a network of portable stand-alone air quality sensor units, and (ii) compile baseline air quality data in six locations downwind of an iron smelting complex in Ile-Ife, Nigeria. However, one limitation of this present work is the use of only linear equations to establish the relationship between meteorological parameters and PM concentrations.

2. Material and methods

2.1. Site description

Ile-Ife, a university town in Southwest Nigeria, has a population of about 502,000 and is characterized by rapid population growth and urban development (Ajala and Olayiwola, 2013). In the recent times, the town has grown from a small center along a number of radial exit roads to a relatively large town. A major road passes through the town and several other paved and unpaved link roads to ease the mobility within the town. On the major road, estimated average vehicular count on weekdays is about 25,000 comprising heavy duty trucks, cars, buses and motorcycles (Owoade et al., 2016).

For this study, six sampling sites were selected in residential communities downwind of an iron smelting facility. These sites include three (3) on the premises of the Obafemi Awolowo University (OAU) campus. The sampling locations were situated at least 2.0 km from one another and at least 0.5 km from the main road. A detailed description (location and nature) of the study sites is highlighted in Table 1. The sites were carefully chosen and evenly distributed to cover residential communities downwind of an iron smelting industry based on the prevailing south-westerly wind. The choice of each location was also based on open space that permits free circulation of air and far from any obstruction that could hinder free flow of air. Figure 1 shows the Google Earth map of the study locations. The climate of the study area is mainly tropical with two distinct seasonal patterns (dry and wet seasons). The dry season runs between November and March while the wet season is from April to October with generally lower temperature and high relative humidity (Jegede et al., 2004).

2.2. Sensors deployment and sampling procedures

The mass concentrations of particulate matter were monitored at five (5) sampling locations using a network of low-cost air quality (AQ) sensors while a high volume Gent sampler was deployed at the sixth location. The sensor nodes used in this study are bespoke low-cost portable air quality devices developed at the Department of Chemistry, University of Cambridge, UK, as part of NERC (Natural Environmental Research Council) funded Sensor Network for Air Quality (SNAQ) project. Details of the fundamental principles and operational procedures of the sensors and in-built atmospheric variables sensors have been reported by Popoola (2012) and Popoola et al. (2018). The fundamental principle of the high volume Gent sampler which utilizes a gravimetric method has been discussed in details by Owoade et al. (2012). The five (5) units of SNAQ boxes were collocated for two weeks (see Figure 2(a)) before deployment to the selected study sites. Figure 2(b) shows the SNAQ unit and Gent sampler deployed downwind of the iron smelting facility.

At each site, the SNAQ unit was mounted at about 3 m above the ground on a 4 m pole and powered with a rechargeable battery. The units were operated simultaneously over a period of 21 days (June 25 – July 15, 2018) at all the locations. The measurements were carried out for 24 h over the entire days of sampling except for the few minutes when the batteries were changed every fortnight. Each unit has an optical particle counter (Alphasense OPC-N2) for monitoring PM number concentration (in size range of 0.38–17.4 μm), these are converted to mass concentration corresponding to the PM metrics $PM_{2.5}$ and PM_{10}. Other measurements made (not presented in this study) include gaseous species; carbon

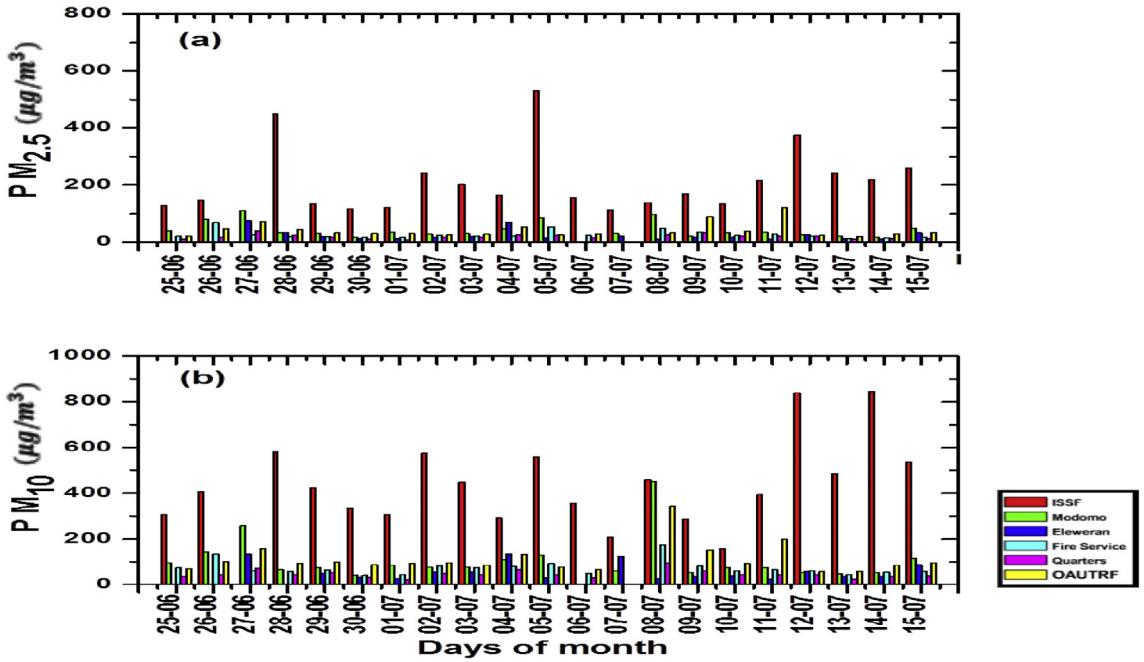

Figure 3. Daily mean concentration of (a) $PM_{2.5}$ and (b) PM_{10} for the months of June and July, 2018.

monoxide (CO), ozone (O_3), nitric oxide (NO), nitrogen dioxide (NO_2) and carbon dioxide (CO_2). Each unit also has inbuilt temperature, relative humidity (RH) sensors as well as a 2D sonic anemometer to measure wind speed and direction. A stacked filter unit Gent high volume sampler was deployed to the ISSF site with the intention to compare the data from the OPC in the sensor unit with that from the Gent sampler. Unfortunately, PM mass concentrations from the Gent sampler had to be used for this site as the OPC became faulty within few hours of deployment. The SNAQ sensor unit records PM concentration and meteorological data every second and then records 20 s averages of the parameters. For continuous measurement, the data were retrieved from the universal serial board stick every fortnight and then undergo further processing with suitable computer packages and software. The PM mass concentrations and meteorological data were averaged to daily resolutions and further statistical analyses were then carried out.

2.3. Optical particle counter (OPC-N2)

The OPC used in this study is manufactured by Alphasense, UK. It is a miniaturized unit measuring 75 mm × 60 mm x 65 mm and weighing about 105 g. This instrument is cheap and portable compared to other high cost reference instrument. The OPC-N2 has a minimum time resolution and capable of sampling particle number concentration over a size range of 0.38–17 μm across 16 size bins and maximum particle count of 10000 s^{-1} through a small fan aspirator. The particle number concentration measured is converted using on-board factory calibration to particle mass concentrations metric for $PM_{2.5}$ and PM_{10}.

2.4. Ambient relative humidity correction for PM concentration

A Gent high-volume sampler was collocated with an OPC-N2 at the ISSF site to monitor PM mass concentrations. The calibration of the OPC was not performed in comparison with the gravimetric high-volume sampler because the OPC became faulty just hours after deployment. As such, the results from this study should be considered indicative. However, the OPC-N2 is known to demonstrate positive artifact in measured particle mass during the periods of high ambient relative humidity (>85 %) which make the raw sensor signals to give an overestimation (several times) of the true PM concentration value. The calibration for particle matter was carried for other study sites using the calibration factor developed based on k-Kohler theory which uses the average bulk particle hygroscopicity (Crilley et al., 2018). The relative humidity effect correction on PM measurement was performed using a correction factor expressed by Crilley et al. (2018) as;

$$C = 1 + \frac{\frac{k}{1.65}}{-1 + \frac{1}{a_w}} \tag{1}$$

$$PM\ (Corrected) = \frac{PM(Raw)}{C} \tag{2}$$

where $a_w = \frac{RH}{100}$ is the water activity, k is a statistical parameter in the range of 0.38–0.41.

2.5. Exponential curves

The exponential curves generated between PM concentrations and meteorological parameter in this study arises as a result of the non-linear relationships which exist between the fit of PM concentrations and meteorological parameters. The non-linearity could be attributed to the demonstration of significant positive artifact in measured particles mass by the OPC during periods of high relative humidity which is due to strong rate of hygroscopic mass growth.

The relationship between the PM concentrations and meteorological parameter is approximated using an exponential function to form the exponential fit equation which is given by;

$$y = Aexp^{\left(\frac{x}{t}\right)} + y_0 \tag{3}$$

where y is the PM concentration, A is a constant, y_0 is the intercept, $\left(\frac{1}{t}\right)$ is the decay rate parameter and x is the meteorological variable such as temperature, relative humidity and wind speed involved in the fit.

2.6. Multiple linear regression (MLR)

Multiple linear regression (MLR) is one of the most important statistical methods used to model the linear relationship between a dependent variable and one or more independent variables. PM con-

Table 2. Statistics of PM mass concentration, air temperature, relative humidity and wind speed results.

Locations	$PM_{2.5}$ (μgm^{-3})		PM_{10} (μgm^{-3})		Air Temperature (°C)		Relative Humidity (%)		Wind Speed (m/s)	
	Range	Mean	Range	Mean	Range	Mean	Range	Mean	Range	Mean
ISSF	112.7–530.8	213.3	156.4–844.6	439.9	19.5–36.0	26.0	14.1–96.6	79.8	0.2–4.4	1.40
Modomo	18.1–110.5	44.1	41.8–451.8	107.1	21.1–35.5	25.6	38.5–90.5	74.9	0.1–3.0	0.93
Eleweran	10.5–77.7	23.8	25.5–134.3	55.0	22.4–35.6	25.8	40.4–93.7	79.0	0.1–2.3	0.87
Fire Service	14.5–67.4	27.7	39.5–175.8	72.4	19.3–36.0	24.3	33.6–96.7	79.0	0.1–2.8	1.03
Staff Quarters	10.2–39.2	20.2	23.0–96.6	45.5	18.4–35.1	23.5	31.2–95.2	74.4	0.1–2.4	0.66
OAUTRF	21.2–121.1	41.5	55.9–344.6	112.0	19.3–35.6	24.8	41.6–94.3	77.1	0.1–2.9	0.77

centrations serve as the dependent variable (or predictand) while meteorological parameters serve as the independent variables (or predictors). The equation for the MLR model is given in Eq. (4):

$$y = a_0 + a_1x_1 + a_2x_2 + a_3x_3 \tag{4}$$

where y is the PM concentration predicted, x_1, x_2 and x_3 are meteorological variables known as descriptors or predictors (temperature, relative humidity and wind speed, respectively).

a_0 is the model constant or intercept and a_1, $a_2$and a_3 are regression coefficients for the meteorological parameters. The regression coefficients represent the independent contributions of each independent variable to the prediction of the dependent variable.

In this study, two statistical indicators - coefficient of determination (R^2) and root mean square error (RMSE) - were employed in the validation of the MLR model.

The coefficient of determination (R^2) account for the total variability proportion in dependent variable (y) that is explained by the regression equation as given by Akpinar et al. (2009) in Eq. (5):

$$R^2 = \frac{\sum \left(y_{pred,i} - \overline{y}\right)^2}{\sum \left(y_{obs,i} - \overline{y}\right)^2} \tag{5}$$

where $\overline{y}$ is the mean value of y, $y_{pred,i}$ is the value of y predicted by the multiple linear regression (MLR) line and $y_{obs,i}$ is the actual measured value of y.

The quality of the fit can be determined using the RMSE which is the standard deviation of the regression line as expressed in Eq. (6):

$$RMSE = \left[\frac{1}{N}\sum \left(y_{pred,i} - y_{obs,i}\right)^2\right]^{\frac{1}{2}} \tag{6}$$

where N is the number of observations.

When the coefficient of determination (R^2) is low, larger RMSE value would be obtained for any regression equations implying poor associated predictions of the dependent variable. If the coefficient of determination (R^2) is high, low RMSE value is expected which indicates that the predictions of the dependent variable (PM) is in close agreement with the measured PM concentrations.

Automatic selection of variables was adopted in the analysis and this was carried out by checking all the model variables with meteorological parameters. Firstly, by looking at the regression linear models of $PM_{2.5}$ and PM_{10} with individual meteorological parameter and then multiple linear regression analysis involving two and later three meteorological parameters as predictor variables for the prediction of PM concentration. This is done to obtain the most accurate and best fitted regression equation for the predictive PM concentration. Although the raw data was obtained at 20 s interval, it was subsequently converted to 30 min average for both dependent and independent variables. This was used as a training data to develop the MLR equations and their predictive performance was assessed using 30 min average dataset which serves as validation data spanning June 25 to July 15, 2018.

3. Results and discussion

3.1. Mass concentrations of the particulate matter

Figure 3a, b show the daily mean concentrations of $PM_{2.5}$ and PM_{10}, respectively. The daily average concentrations of $PM_{2.5}$ and PM_{10} are 213.3, 44.1, 23.8, 27.7, 20.2 and 41.5 μg/m^3 and 439.9, 107.1, 55.0, 72.4, 45.5 and 112.0 μg/m^3 at ISSF, Modomo, Eleweran, Fire Service, staff quarters and OAUTRF, respectively. At ISSF, the range of daily mean concentrations of $PM_{2.5}$ and PM_{10} are 112.7–530.8 μg/m^3 and 156.4–844.6 μg/m^3, respectively (see Table 2). These high concentrations of PM at the ISSF sampling site are attributable to its proximity to the Iron and steel smelting factory.

US EPA's National Ambient Air Quality Standard (NAAQS) and United States Air Quality Standard (US AQS) threshold limits of 35 and 150 μg/m^3 for $PM_{2.5}$ and PM_{10} for daily averages were exceeded at ISSF, Modomo and OAUTRF. The high PM concentration observed at Modomo was noticed in the polar plot in Figure 3. These are related to emissions from the iron and steel factory where high temperature processing of scrap metals is carried out with electric arc furnaces (EAF) (Owoade et al., 2015). The data for June 25 and 26 at Eleweran site were not included in the analysis due to the malfunctioning of the units on these days. Except on some few days, PM concentrations at Eleweran were below the NAAQS threshold limit for daily average concentration. The lower concentration of $PM_{2.5}$ at Eleweran could be attributed to the fact that the area is a developing remote residential area with few anthropogenic activities. The daily mean mass concentrations of PM at OAUTRF were higher than the ones observed in the staff quarters. Apart from traffic activities on the paved road and small-scale refuse burning in the staff quarters, there are no major anthropogenic activities that could contribute to the PM concentration in the staff quarters. However, tractors, plough and other farm implement occasional work on the University research farm close to the OAUTRF sampling site.

3.2. Temporal variation of particulate matter concentration and meteorological variables

Mean values of meteorological variables for the six (6) sampling sites are presented in Table 2. The range of daytime mean values of wind speed, relative humidity and air temperature are 0.7–1.1 m/s, 67–78 % and 24–27 °C, respectively, while nighttime mean values range from 0.5-0.9 m/s, 79–84 % and 22–25 °C, respectively. It was observed that air temperature increases with an increase in wind speed during the daytime resulting in lower relative humidity and PM mass concentrations. Increase in wind speed promotes the dispersion while moderate or high temperature results in atmospheric instability and high mobility of particle in the atmosphere, leading to reduction in particulate matter concentrations (Abiye, 2015). The increase in atmospheric instability resulting from high temperature could leads to a higher boundary layer (Pahlow et al., 2001). During nighttime, high relative humidity was observed while air temperature was lower in values with higher PM concentrations. This might be due to the shallow nocturnal boundary

Table 3. Summary of the daytime and nighttime relationship between particulate matter ($PM_{2.5}$ and PM_{10}) and meteorological variables.

Locations	Particulate Matter	Wind Speed (R^2)		Temperature (R^2)		Relative Humidity (R^2)	
		Daytime	Nighttime	Daytime	Nighttime	Daytime	Nighttime
Modomo	$PM_{2.5}$	0.07	0.17	0.27	0.38	0.49	0.40
	PM_{10}	0.09	0.07	0.25	0.24	0.37	0.18
Eleweran	$PM_{2.5}$	0.06	0.08	0.07	0.09	0.15	0.24
	PM_{10}	0.04	0.06	0.07	0.16	0.13	0.16
Fire Service	$PM_{2.5}$	0.09	0.11	0.06	0.31	0.09	0.39
	PM_{10}	0.03	0.03	0.01	0.15	0.02	0.12
Staff Quarters	$PM_{2.5}$	0.15	0.17	0.13	0.11	0.21	0.28
	PM_{10}	0.08	0.06	0.12	0.09	0.16	0.11
OAUTRF	$PM_{2.5}$	0.18	0.16	0.17	0.11	0.29	0.23
	PM_{10}	0.19	0.04	0.25	0.23	0.36	0.09

layer with characteristic stable atmospheric condition which impedes the dispersion of particles, hence leading to a build-up of PM concentration.

The strong relationship observed with greater PM concentrations for RH > 80 % for both day and nighttime periods could be attributed to hygroscopic particle growth which occurred when the deliquescence relative humidity is exceeded. Similar relationships between RH and PM concentrations have been established in a number of studies, for example, Crilley et al. (2018) and Di Antonio et al. (2018). The evaluation of low-cost OPC carried out in a background site in the UK by Crilley et al. (2018) established that a threshold of RH > 85% is needed for a significant impact on PM concentration to be observed.

The statistics of the concentrations of PM and meteorological variables at the six sampling sites are presented in Table 2. A negative exponential distribution curves (decay curve) were obtained for the relationship between PM concentrations and meteorological variables at the sampling sites. The coefficient of determination (R^2) values ranged from 0.03-0.19 and 0.03–0.17 for day and nighttime, respectively. The nighttime and daytime decay curves are shown in Figure S1(a - l) in the supplementary material. The lower R^2 values between PM concentration and wind speed indicates the dominance of local sources (Sumesh et al., 2017). The decay curves illustrate inverse variation between PM concentration and wind speed. Strong winds enhances the dispersion of PM and low winds allow pollution levels to rise in the atmosphere (Li et al., 2014; Owoade et al., 2012). In their study, Whiteman et al. (2014) found that ambient PM concentrations are inversely proportional to wind speed. Similar to the relationship between PM concentration and wind

Table 4. Linear Regression (LR) relationship for one meteorological variable predictor.

Location		Multiple Regression Equations	R^2	RMSE ($\mu g/m^3$)	Measured Value ($\mu g/m^3$)	Predicted Value ($\mu g/m^3$)
Modomo	T	$PM_{2.5}$ = 284.47–9.37T	0.20	59.56	44.10	44.17
		PM_{10} = 720.21–23.89T	0.07	267.62	107.10	107.58
	RH	$PM_{2.5}$ = 2.21–120.65RH	0.21	59.05	44.10	43.89
		PM_{10} = 5.42RH-296.32	0.07	267.75	107.10	106.27
	ws	$PM_{2.5}$ = 85.62–43.35ws	0.11	62.54	44.10	44.55
		PM_{10} = 220.79–118.60ws	0.05	271.11	107.10	109.25
Eleweran	T	$PM_{2.5}$ = 93.82–2.72T	0.07	30.85	23.79	23.85
		PM_{10} = 231.31–6.86T	0.07	79.73	54.97	55.13
	RH	$PM_{2.5}$ = 0.71RH-31.89	0.10	30.37	23.79	23.70
		PM_{10} = 1.62RH-71.01	0.08	79.32	54.97	54.74
	ws	$PM_{2.5}$ = 41.12–20.31ws	0.07	30.88	23.79	24.02
		PM_{10} = 95.05–46.97ws	0.05	80.22	54.97	55.57
Fire Service	T	$PM_{2.5}$ = 110.74–3.44T	0.11	32.17	27.65	27.73
		PM_{10} = 199.79–5.27T	0.02	111.34	72.42	72.66
	RH	$PM_{2.5}$ = 0.76RH-32.30	0.12	31.95	27.65	27.56
		PM_{10} = 1.11RH +15.62	0.02	111.31	72.42	72.07
	ws	$PM_{2.5}$ = 50.32–21.73ws	0.09	32.37	27.65	27.89
		PM_{10} = 111.17–37.17ws	0.03	111.19	72.42	73.21
Staff Quarters	T	$PM_{2.5}$ = 76.23–2.40T	0.14	20.53	20.24	20.29
		PM_{10} = 169.50–5.30T	0.09	59.49	45.48	45.62
	RH	$PM_{2.5}$ = 0.60RH-24.79	0.18	20.08	20.24	20.18
		PM_{10} = 1.27RH-49.36	0.10	59.08	45.48	45.28
	ws	$PM_{2.5}$ = 40.37–30.94ws	0.16	20.21	20.24	20.38
		PM_{10} = 83.59–58.57ws	0.07	59.86	45.48	45.89
OAUTRF	T	$PM_{2.5}$ = 182.5–5.71T	0.16	43.52	41.54	41.64
		PM_{10} = 539.14–17.29T	0.06	229.62	112.02	112.52
	RH	$PM_{2.5}$ = 1.52RH-76.48	0.21	42.43	41.54	41.42
		PM_{10} = 4.14RH-208.65	0.06	229.56	112.02	111.35
	ws	$PM_{2.5}$ = 82.14–55.00ws	0.17	43.32	41.54	41.86
		PM_{10} = 220.83–147.40ws	0.05	230.96	112.02	113.73

Table 5. Multiple Linear Regression (MLR) relationship for two meteorological variables predictor.

Location		Multiple Regression Equations	R^2	RMSE (μg/m^3)	Measured Value (μg/m^3)	Predicted Value (μg/m^3)
Modomo	T, RH	$PM_{2.5}$ = 7.07T + 3.80RH-420.64	0.21	58.96	44.10	44.56
		PM_{10} = 448.18–17.55T + 1.47RH	0.07	267.74	107.10	124.17
	T, ws	$PM_{2.5}$ = 261.47–7.76T-18.97ws	0.21	59.00	44.10	38.26
		PM_{10} = 648.25–18.87T-59.34ws	0.08	266.48	107.10	80.89
	RH, ws	$PM_{2.5}$ = 1.90RH-14.99ws-82.87	0.22	58.73	44.10	36.85
		PM_{10} = 4.27RH-54.83ws-158.12	0.08	266.87	107.10	74.34
Eleweran	T, RH	$PM_{2.5}$ = 14.79T + 3.87RH-661.73	0.16	29.29	23.79	24.07
		PM_{10} = 11.46T + 4.05RH-558.96	0.08	79.12	54.97	55.74
	T, ws	$PM_{2.5}$ = 80.70–1.79T-12.92ws	0.09	30.55	23.79	19.52
		PM_{10} = 204.33–4.93T-26.58ws	0.08	79.25	54.97	45.60
	RH, ws	$PM_{2.5}$ = 0.55RH-9.61ws-11.44	0.11	30.22	23.79	20.18
		PM_{10} = 1.22RH-23.23ws-21.57	0.08	78.98	54.97	43.81
Fire Service	T, RH	$PM_{2.5}$ = 4.33T + 1.64RH-207.26	0.12	31.87	27.65	27.93
		PM_{10} = 0.67T + 0.97RH-11.57	0.03	111.36	72.42	78.74
	T, ws	$PM_{2.5}$ = 98.00–2.36T-12.87ws	0.13	31.78	27.65	23.83
		PM_{10} = 174.68–3.14T-25.36ws	0.03	110.94	72.42	59.06
	RH, ws	$PM_{2.5}$ = 0.55RH-11.50ws-3.83	0.14	31.64	27.65	23.00
		PM_{10} = 0.66RH-24.82ws+45.81	0.03	110.94	72.42	114.82
Staff Quarters	T, RH	$PM_{2.5}$ = 10.25T + 2.85RH-432.64	0.24	19.26	20.24	20.38
		PM_{10} = 11.66T + 3.83RH-512.97	0.11	58.75	45.48	45.91
	T, ws	$PM_{2.5}$ = 66.39–1.36T-21.96ws	0.20	19.84	20.24	17.83
		PM_{10} = 155.16–3.70T-34.24ws	0.10	58.95	45.48	38.31
	RH, ws	$PM_{2.5}$ = 0.40RH-18.82ws+2.58	0.22	19.58	20.24	27.23
		PM_{10} = 0.95RH-29.89ws+5.89	0.11	58.68	45.48	36.60
OAUTRF	T, RH	$PM_{2.5}$ = 14.63T + 4.94RH-703.04	0.25	41.33	41.54	41.95
		PM_{10} = -6.85T + 2.54RH-184.69	0.06	229.63	112.02	135.28
	T, ws	$PM_{2.5}$ = 157.77–3.61T-36.65ws	0.22	42.12	41.54	36.88
		PM_{10} = 482.42–12.48T-83.94ws	0.07	228.34	112.02	86.76
	RH, ws	$PM_{2.5}$ = 1.09RH-31.41ws-19.53	0.24	41.39	41.54	36.00
		PM_{10} = 2.99RH-82.44ws-59.14	0.07	228.35	112.02	81.41

speed, a negative exponential decay curve was observed between PM and temperature in all the sampling sites. The ranges of R^2 values for daytime and nighttime were 0.01–0.27 and 0.09–0.38. The difference in R^2 values could be attributed to impact of diurnal temperature variation of the PM concentration.

A more dynamically unstable boundary layer (compared to nighttime) is often characteristic of daytime which favours effective dispersion of atmospheric pollutants; hence, lowering ambient PM concentrations. In contrast, calm condition and lower temperature limit the free mixing of PM during night time, resulting in high PM concentration (Li et al., 2017). At low temperatures, an elevated PM level occurred indicating the reduced vertical and horizontal mixing due to the stable atmospheric conditions which limits the dispersion of air pollutants. An exponential relationship is observed between PM and relative humidity with R^2 value ranges of 0.02–0.49 and 0.09–0.40 for daytime and nighttime periods, respectively. The small variation in R^2 values might be as a result of the scavenging effect of the PM concentration. A summary of R^2 values for the relationship between PM concentrations and meteorological variables during daytime and nighttime at five (5) sampling sites are presented in Table 3. During nighttime, dispersion of air pollutants might be prevented, resulting in the suspension of PM near the vicinity of the observation site while during the daytime, relatively low humidity values promotes dilution of PM, leading to lower concentrations (Sumesh et al., 2017). The low coefficient of determinations observed for different exponential fits in Figures S1(a - l) is an indication that there was a weak relationship between the PM concentrations and meteorological variables at the sampling sites.

Table 6. Multiple Linear Regression (MLR) relationship for three meteorological variables predictor.

Location		Multiple Regression Equations	R^2	RMSE (μg/m^3)	Measured Value (μg/m^3)	Predicted Value (μg/m^3)
Modomo	$PM_{2.5}$	$PM_{2.5}$ = 4.05T + 2.84RH – 13.68ws – 258.15	0.22	58.73	44.10	38.88
	PM_{10}	PM_{10} = 1222.67–31.93T -3.14RH – 65.19ws	0.08	266.54	107.10	90.28
Eleweran	$PM_{2.5}$	$PM_{2.5}$ = 14.67T + 3.70RH – 9.08ws – 637.11	0.18	29.15	23.79	21.55
	PM_{10}	PM_{10} = 11.15T + 3.61RH – 22.83ws – 497.08	0.09	78.78	54.97	48.92
Fire Service	$PM_{2.5}$	$PM_{2.5}$ = 3.87T + 1.35RH – 11.16ws – 161.01	0.14	31.58	27.65	24.99
	PM_{10}	PM_{10} = -1.70T + 0.31RH – 24.97ws + 115.02	0.03	110.99	72.42	102.83
Staff Quarters	$PM_{2.5}$	$PM_{2.5}$ = 9.87T + 2.58RH – 17.63ws -391.57	0.28	18.80	20.24	18.59
	PM_{10}	PM_{10} = 11.03T + 3.38RH – 28.56ws – 446.44	0.12	58.38	45.48	40.34
OAUTRF	$PM_{2.5}$	$PM_{2.5}$ = 14.74T + 4.53RH – 31.65ws – 650.24	0.29	40.26	41.54	38.68
	PM_{10}	PM_{10} = 1.46RH –6.57T-82.34ws – 222.05	0.07	228.43	112.02	134.16

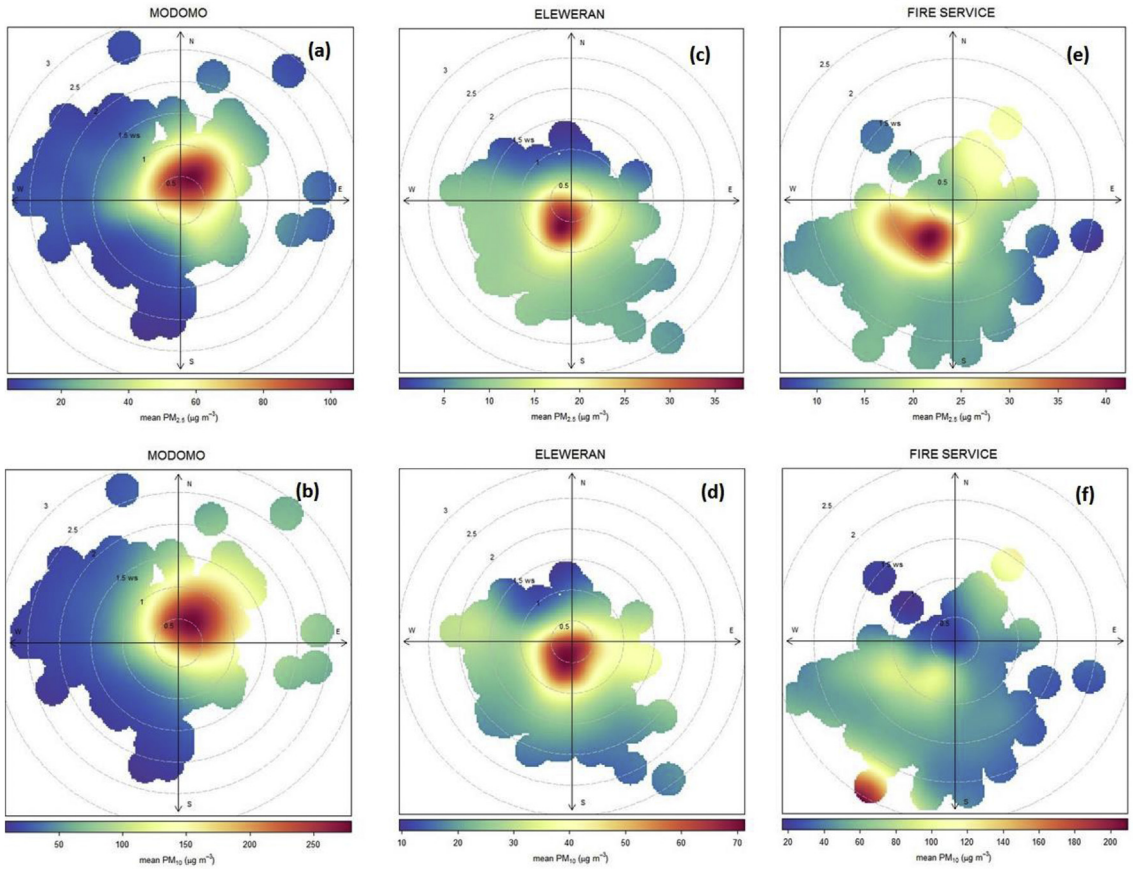

Figure 4. Bivariate polar plots of PM at Modomo, Eleweran and Fire service stations.

3.3. Multiple linear regression analysis

Tables 4, 5, and 6 present the regression equations, coefficients of determination (R^2), root mean square error (RMSE) using automatic selection of variables method for the prediction of $PM_{2.5}$ and PM_{10} in five sampling locations. Table 4 shows that the coefficient of determination (R^2) of the statistical model of $PM_{2.5}$ using one meteorological variable range from 0.07 - 0.20, 0.10–0.21 and 0.07–0.17 for temperature, RH and wind speed, respectively. The coefficient of determination (R^2) obtained from the model of PM_{10} using one meteorological variable range from 0.02 - 0.09, 0.02–0.10 and 0.03–0.07 for temperature, RH and wind speed, respectively. A mix of weak and moderate correlations between PM concentrations and meteorological variables can be observed from Table 4.

Low coefficient of determination (R^2) recorded in Table 4 suggests that other variables contributing to the variability of PM should be considered simultaneously because the relationship between the PM and meteorological variables are not adequately understood. Therefore, multiple linear regression analysis involving two meteorological variables as predictor variables was carried out and the results are presented in Table 5. The results of the MLR showed that the coefficient of determination (R^2) for $PM_{2.5}$ prediction using temperature and RH, temperature and wind speed, and RH and wind speed ranged from 0.12-0.25, 0.09–0.22 and 0.11–0.24, respectively (see Table 5). There was significant improvement in the coefficient of determination (R^2) recorded in Table 5 when compared with result in Table 4 where individual meteorological variable was used as predictor variable for $PM_{2.5}$.

It can be concluded that the combination of other meteorological parameter with wind speed in the MLR equations is responsible for the improvement in the coefficient of determination (R^2) (Table 5). As shown in Table 5, temperature and RH are both responsible for 21%, 16%, 12%, 24% and 25% in variation of $PM_{2.5}$ at Modomo, Eleweran, Fire Service, Staff Quarters and OAUTRF, respectively. RMSE values for the estimated values are 58.96, 29.29, 31.87, 19.26 and 41.33 in order for the five locations. Temperature and wind speed both account for 21%, 9%, 13%, 20% and 22% in variation of $PM_{2.5}$ and RMSE values for the estimations are 59.00, 30.55, 31.78, 19.84 and 42.12 at Modomo, Eleweran, Fire Service, Staff Quarters and OAUTRF, respectively. RH and wind speed both account for 22%, 11%, 14%, 22% and 24% variation in $PM_{2.5}$ at Modomo, Eleweran, Fire Service, Staff Quarters and OAUTRF, respectively. The RMSE values for the estimations are 58.73, 30.22, 31.64, 19.58 and 41.39 in order for the five locations. The results showed that while RH and wind speed jointly contribute mostly to changes in $PM_{2.5}$ at Modomo and Fire Service, temperature and RH are the greatest determinants of changes in $PM_{2.5}$ at Eleweran, Staff Quarters and OAUTRF.

It was observed that the two independent variables (temperature and RH) in the MLR model had positive regression coefficients with negative intercept. This is an indication that the increase in PM concentration is associated with increase in any of the predictor variable. Also, the model equations when temperature and wind speed were used as predictor variable indicated negative regression coefficients for all the sampling locations. This is an indication that increases in both temperature and wind speed will spread away the PM pollutants and increase their buoyancy thus reducing predicted PM concentrations. The inclusion of two meteorological variables as predictor variables in the MLR model slightly improved the R^2 value in Table 5 but fail to explain the MLR model fully.

Three meteorological variables were considered as predictor variables to further test the workability of the MLR model at the sampling sites. The results of the MLR model with three meteorological variables as predictor are presented in Table 6. The MLR analysis modeled the relationship between PM mass concentrations (criterion variable) and RH,

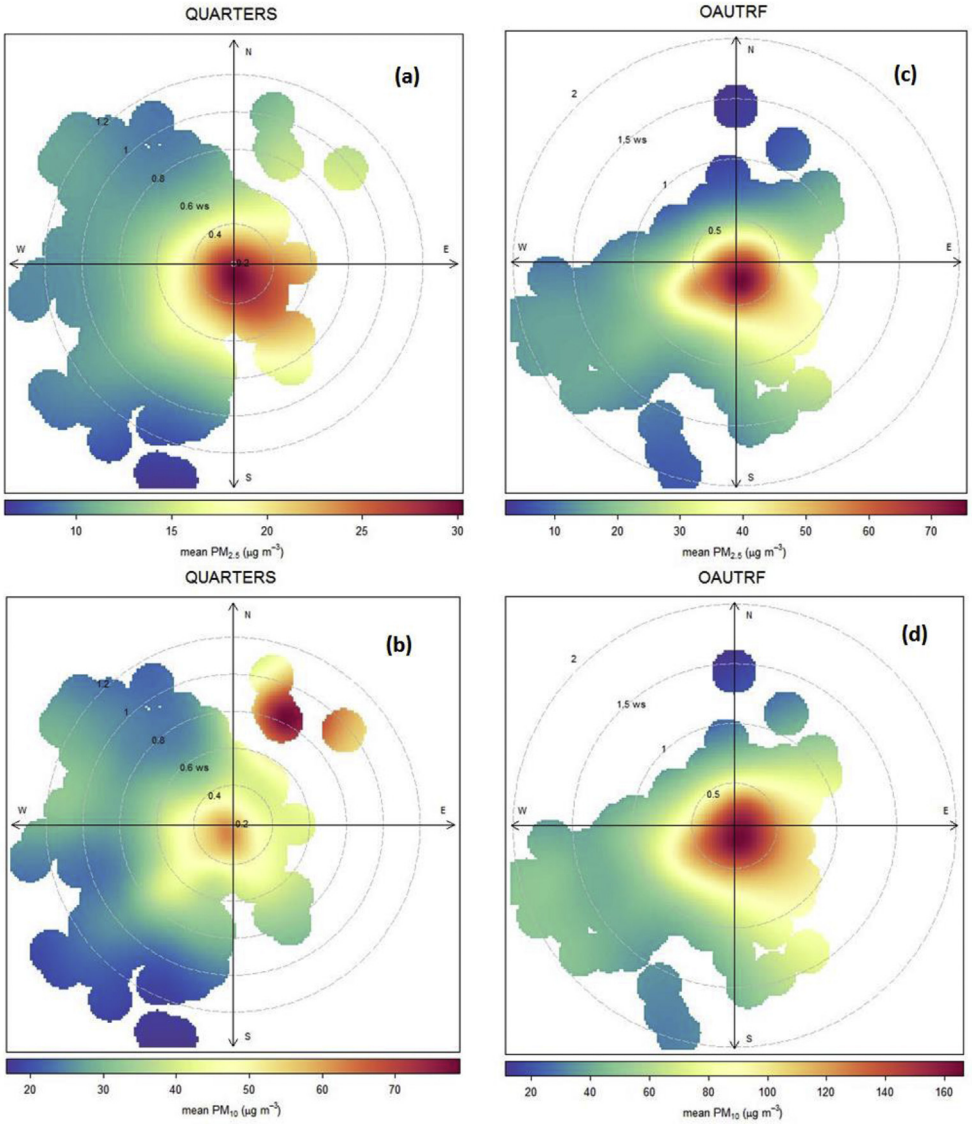

Figure 5. Bivariate polar plots of PM at Staff Quarters and OAUTRF Stations.

wind speed and air temperature (predictor variables) by fitting a linear equation to the observed data. The coefficient of determination (R^2) values of $PM_{2.5}$ and PM_{10} are 0.28 and 0.12 for OAURTF, and 0.29 and 0.07 for staff quarter, respectively. The R^2 values of the other sites are also low but the RMSE values of $PM_{2.5}$ and PM_{10} of the predicted value relative to observations are 29.15 and 18.80 µg/m^3 for Eleweran and Staff quarter, respectively. The predicted means of PM_{10} mass concentration using MLR model were slightly greater than the observed PM_{10} mean values by 41.19 and 19.76 % at Fire service and OAUTRF, respectively. The model underestimated PM_{10} concentration measured at Modomo, Eleweran and Staff quarters by 15.70, 11.01 and 11.30%.

Temperature, RH and wind speed, as shown in Table 6, jointly account for 22%, 17%, 14%, 28% and 29 % of a variation in $PM_{2.5}$ at Modomo, Eleweran, Fire Service, Staff Quarters and OAUTRF, respectively. RMSE values of 58.73, 29.15, 31.58, 18.8 and 40.26 are obtained for the sites in the order above. Also, temperature, RH and wind speed jointly account for 8%, 9%, 3%, 12% and 7 % of a variation in PM_{10} at Modomo, Eleweran, Fire Service, Staff Quarters and OAUTRF, respectively. This goes with RMSE of about 266.54, 78.78, 110.99, 58.38 and 228.43 for each location in the order above. The results showed that the fit was better for $PM_{2.5}$ than for PM_{10} which is an indication that temperature, relative humidity and wind speed explain changes in $PM_{2.5}$ better than PM_{10} concentrations.

3.4. Bivariate concentration polar plots

Figures 4 and 5 show the bivariate polar plots of $PM_{2.5}$ and PM_{10} at the sampling sites. Bipolar plot shows the directional influence of wind on PM concentrations. In the plots, PM concentrations showed substantial variations accompanied with low wind speed (0–2 m/s) in all the wind sectors in the sampling sites. The moderate $PM_{2.5}$ concentration observed at Modomo (Figure 4a) and Staff Quarters (Figure 5a) in the Northwesterly and Northeasterly directions (ws $>$ 0.5 m/s) shows a prevailing wind blowing across these sites transporting PM from the local sources, most especially the iron smelting factory and refuse burning activities located southeasterly and southwesterly of Modomo and Staff quarters sites, respectively. The occurrence of elevated $PM_{2.5}$ mass concentrations in all directions suggest that there were other local sources of $PM_{2.5}$ near the sampling sites apart from the iron smelting factory in the northeasterly direction. This local source of fine PM fraction could be the unpaved road network around the sampling sites. In Figures 4 and 5, bipolar plots for PM_{10} shows the directional dependence of high PM_{10} occurring at low wind speed along Northeasterly direction while slightly

low concentrations of $PM_{2.5}$ and PM_{10} concentrations were observed at wind speed >1.5 m/s in the Northwesterly and Northeasterly directions at Modomo site. Higher PM_{10} mass concentrations at low wind speed were noticed at Eleweran in all directions. At Fire station sampling site and for wind speed >1 m/s, PM_{10} mass concentration are very high in the North-western direction (see Figure 4f). At Staff quarters and OAUTRF sites, the bivariate polar plots in Figure 5 indicate that the elevated PM_{10} mass concentrations occurred when wind speeds >0.5 m/s along the Northeasterly directions at the Staff quarters site. Generally, the elevated $PM_{2.5}$ and PM_{10} mass concentrations at low wind speeds (which indicates a stable atmospheric condition) suggest that pollution episode might likely occurred under this condition due to the inhibition of PM pollutants dispersion in the affected wind direction. At high wind speed, the elevated $PM_{2.5}$ and PM_{10} mass concentrations pose no threat because as the particles are suspended, they are dispersed immediately due to the unstable nature of the atmosphere which enhances the dispersion of PM pollutants.

4. Conclusion

This study presents mass concentrations of particulate matter and meteorological parameters (wind speed, wind direction, air temperature and relative humidity) measured simultaneously at six sampling locations in Ile-Ife using a network of low-cost air quality sensor units. The highest daily average values of $PM_{2.5}$ and PM_{10} are 530.81 and 844.58 $\mu g/m^3$, respectively and were observed at ISSF site while the lowest daily mean values of 0.39 and 1.25 $\mu g/m^3$ were observed for $PM_{2.5}$ and PM_{10}, respectively at Eleweran. A negative exponential distribution curve was obtained for the relationship between PM and wind speed with coefficient of determination (R^2) values ranging from 0.06 - 0.18 for $PM_{2.5}$ and 0.03–0.19 for PM_{10} during daytime and nighttime periods in all the sampling sites. The relationship between PM and temperature gave a decay curve which show that high PM concentrations are associated with lower temperature while RH had an exponential growth curve with PM concentrations increasing with RH increase. A multivariate linear regression (MLR) equation was developed for the relationship between PM and meteorological variables. This study demonstrates the strength and potential of miniaturized novel low-cost air quality monitoring sensors in providing measurement-based evidence that could help address some of the air pollution challenges in developing economies, especially the serious dearth of 24-h continuous AQ data. This will not only assist policy makers and environmental agencies in monitoring the effectiveness of existing control measures but also facilitate the introduction of new interventions as and at when needed. However, further studies involving the use of other statistical models other than linear equations and utilizing more meteorological variables is recommended to improve the model matching.

Declarations

Author contribution statement

Opeyemi Omokungbe, Oyediran K. Owoade, Felix S. Olise: Conceived and designed the experiments; Performed the experiments; Wrote the paper.

Olusegun G. Fawole: Conceived and designed the experiments; Performed the experiments; Analyzed and interpreted the data; Wrote the paper.

Muritala A. Ayoola, Adekunle B. Toyeje, Ayodele P. Olufemi, Pelumi O. Abiodun, Olawale E. Abiye, Lukman A. Sunmonu: Performed the experiments; Analyzed and interpreted the data; Wrote the paper.

Olalekan A.M. Popoola, Roderic L. Jones: Conceived and designed the experiments; Analyzed and interpreted the data; Wrote the paper.

Funding statement

This research did not receive any specific grant from funding agencies in the public, commercial, or not-for-profit sectors.

Competing interest statement

The authors declare no conflict of interest.

Additional information

Supplementary content related to this article has been published online at https://doi.org/10.1016/j.heliyon.2020.e04207.

Acknowledgements

The authors are grateful to the Department of Chemistry, University of Cambridge for providing the units of low-cost air quality sensor used in this study. We will also like to appreciate the Atmospheric Physics Research Group (APRG) of the Department of Physics and Engineering Physics, Obafemi Awolowo University, Ile-Ife, Nigeria for providing space for the deployment of the units on the OAUTRF and the provision of meteorological data from reference instruments in the meteorological station in OAUTRF to calibrate the units.

References

Abiye, O., 2015. Meteorological Modeling of Atmospheric Dispersal of Gaseous Effluents from a Scrap-Iron Recycling Factory at Ile-Ife, SouthWest Nigeria. Obafemei Awolowo University, Nigeria.

Ajala, O., Olayiwola, A., 2013. An assessment of the growth of Ile-Ife, Osun state Nigeria, using multi-temporal imageries. J. Geogr. Geol. 5 (2), 43.

Akpinar, E.K., Akpinar, S., Öztop, H.F., 2009. Statistical analysis of meteorological factors and air pollution at winter months in Elaziğ, Turkey. J. Urban Environ. Eng. 3 (1), 7–16.

Ancelet, T., Davy, P.K., Trompetter, W.J., Markwitz, A., Weatherburn, D.C., 2011. Carbonaceous aerosols in an urban tunnel. Atmos. Environ. 45 (26), 4463–4469.

Chakraborty, S., Fu, R., Massie, S.T., Stephens, G., 2016. Relative influence of meteorological conditions and aerosols on the lifetime of mesoscale convective systems. Proc. Natl. Acad. Sci. Unit. States Am. 113 (27), 7426–7431.

Chakraborty, S., Fu, R., Rosenfeld, D., Massie, S.T., 2018. The influence of aerosols and meteorological conditions on the total rain volume of the mesoscale convective systems over tropical continents. Geophys. Res. Lett. 45 (23), 13,099–13,106.

Crilley, L.R., Shaw, M., Pound, R., Kramer, L.J., Price, R., Young, S., Lewis, A.C., Pope, F.D., 2018. Evaluation of a low-cost optical particle counter (Alphasense OPC-N2) for ambient air monitoring. Atmos. Meas. Tech. 709–720.

Di Antonio, A., Popoola, O.A., Ouyang, B., Saffell, J., Jones, R.L., 2018. Developing a relative humidity correction for low-cost sensors measuring ambient particulate matter. Sensors 18 (9), 2790.

Galindo, N., Yubero, E., Nicolás, J., Crespo, J., Pastor, C., Carratalá, A., Santacatalina, M., 2011. Water-soluble ions measured in fine particulate matter next to cement works. Atmos. Environ. 45 (12), 2043–2049.

Gogikar, P., Tyagi, B., Padhan, R.R., Mahaling, M., 2018. Particulate matter assessment using in situ observations from 2009 to 2014 over an industrial region of eastern India. Earth Syst. Environ. 2 (2), 305–322.

Haque, M.M., Kawamura, K., Kim, Y., 2016. Seasonal variations of biogenic secondary organic aerosol tracers in ambient aerosols from Alaska. Atmos. Environ. 130, 95–104.

Harrison, R.M. (Ed.), 2014. Air Pollution: Sources, Concentrations and Measurements. Pollution: Causes, Effects and Control. Royal Society of Chemistry, United Kingdom, pp. 157–181.

Harrison, R.M., 2015. Pollution: Causes, Effects and Control. Royal Society of Chemistry.

Hu, R., Wang, H., Yin, Y., Zhu, B., Xia, L., Zhang, Z., Chen, K., 2018. Measurement of ambient aerosols by single particle mass spectrometry in the Yangtze River Delta, China: seasonal variations, mixing state and meteorological effects. Atmos. Res. 213, 562–575.

Jayamurugan, R., Kumaravel, B., Palanivelraja, S., Chockalingam, M., 2013. Influence of temperature, relative humidity and seasonal variability on ambient air quality in a coastal urban area. Int. J. Atmos. Sci. 2013.

Jegede, O., Maunder, M., Okogbue, E., Foken, T., Balogun, E., Adedokun, J., Oladiran, E., Omotosho, J., Balogun, A., Oladosu, O., 2004. The Nigerian micrometeorological experiment (NIMEX-1): an overview. IFE J. Sci. 6 (2), 191–202.

Li, L., Qian, J., Ou, C.-Q., Zhou, Y.-X., Guo, C., Guo, Y., 2014. Spatial and temporal analysis of Air Pollution Index and its timescale-dependent relationship with

meteorological factors in Guangzhou, China, 2001–2011. Environ. Pollut. 190, 75–81.
Li, X., Feng, Y., Liang, H., 2017. The impact of meteorological factors on PM2. 5 variations in Hong Kong. In: IOP Conference Series: Earth and Environmental Science. IOP Publishing, p. 12003.
Lin, H., Liu, T., Xiao, J., Zeng, W., Li, X., Guo, L., Xu, Y., Zhang, Y., Vaughn, M.G., Nelson, E.J., 2016. Quantifying short-term and long-term health benefits of attaining ambient fine particulate pollution standards in Guangzhou, China. Atmos. Environ. 137, 38–44.
Mahapatra, P., Sinha, P., Boopathy, R., Das, T., Mohanty, S., Sahu, S., Gurjar, B., 2018. Seasonal progression of atmospheric particulate matter over an urban coastal region in peninsular India: role of local meteorology and long-range transport. Atmos. Res. 199, 145–158.
Mohan, S.M., 2016. An overview of particulate dry deposition: measuring methods, deposition velocity and controlling factors. Int. J. Environ. Sci. Technol. 13 (1), 387–402.
Owoade, Olise, F.S., Ogundele, L.T., Fawole, O.G., Olaniyi, H.B., 2012. Correlation between particulate matter concentration and meteorological parameter at a site in Ile-Ife, Nigeria. IFE J. Sci. 14 (1), 83–93.
Owoade, K.O., Hopke, P.K., Olise, F.S., Adewole, O.O., Ogundele, L.T., Fawole, O.G., 2016. Source apportionment analyses for fine (PM 2.5) and coarse (PM 2.5–10) mode particulate matter (PM) measured in an urban area in southwestern Nigeria. Atmos. Pollut. Res. 7 (5), 843–857.
Owoade, O.K., Hopke, P.K., Olise, F.S., Ogundele, L.T., Fawole, O.G., Olaniyi, B.H., Jegede, O.O., Ayoola, M.A., Bashiru, M.I., 2015. Chemical compositions and source identification of particulate matter (PM2.5 and PM2.5–10) from a scrap iron and steel smelting industry along the Ife–Ibadan highway, Nigeria. Atmos. Pollut. Res. 6 (1), 107–119.
Pahlow, M., Parlange, M.B., Porté-Agel, F., 2001. On Monin–Obukhov similarity in the stable atmospheric boundary layer. Boundary-Layer Meteorol. 99 (2), 225–248.
Popoola, O.A., Carruthers, D., Lad, C., Bright, V.B., Mead, I.M., Stettler, M., Saffell, J., Jones, R.L., 2018. The use of networks of low cost air quality sensors to quantify air quality in urban settings. Atmos. Environ. 194, 58–70.
Popoola, O.A.M., 2012. Studies of Urban Air Quality Using Electrochemical Based Sensor Instruments. University of Cambridge, UK.
Seinfeld, J.H., Pandis, S.N., 2016. Atmospheric Chemistry and Physics: from Air Pollution to Climate Change. John Wiley & Sons.
Sturm, R., 2012. Theoretical models of carcinogenic particle deposition and clearance in children's lungs. J. Thorac. Dis. 4 (4), 368.
Sumesh, R., Rajeevan, K., Resmi, E., Unnikrishnan, C., 2017. Particulate matter concentrations in the southern tip of India: temporal variation, meteorological influences, and source identification. Earth Syst. Environ. 1 (2), 13.
Whiteman, C.D., Hoch, S.W., Horel, J.D., Charland, A., 2014. Relationship between particulate air pollution and meteorological variables in Utah's Salt Lake Valley. Atmos. Environ. 94, 742–753.
Zu, Y., Huang, L., Hu, J., Zhao, Z., Liu, H., Zhang, H., Ying, Q., Chen, M., 2017. Investigation of relationships between meteorological conditions and high PM 10 pollution in a megacity in the western Yangtze River Delta, China. Air Qual. Atmos. Health 10 (6), 713–724.
Żyromski, A., Biniak-Pieróg, M., Burszta-Adamiak, E., Zamiar, Z., 2014. Evaluation of relationship between air pollutant concentration and meteorological elements in winter months. J. Water Land Dev. 22 (1), 25–32.